



Cite this: *RSC Adv.*, 2017, 7, 49605

CuO/V₂O₅ hybrid nanowires for highly sensitive and selective H₂S gas sensor†

Bu-Yu Yeh,^a Bo-Sung Jian,^a Gou-Jen Wang ^b and Wenjea J. Tseng ^{*a}

Vanadium pentoxide (V₂O₅) nanowires decorated with CuO nanoparticles on their surface have been prepared by a facile chemical route. The gas-sensing performance of the CuO/V₂O₅ nanohybrids has been examined against H₂S, CO, and NO₂ gases over a range of gas concentrations from 7 to 60 ppm and working temperatures from 100 to 400 °C, and compared with that of pristine V₂O₅ nanowires without the decoration. The CuO/V₂O₅ nanohybrids exhibit a greatly enhanced sensitivity toward H₂S gas selectively and are relatively indifferent to CO and NO₂ gases. The gas-sensing response of the nanohybrids increases by nearly 18 times (from 1.84 to 31.86) when tested against 23 ppm of H₂S gas at 220 °C. The nanohybrids remain stable when detecting H₂S gas for a period of two weeks. This selective enhancement is attributable to the local p–n junction formed at the interface together with the reversible chemical reaction that occurs when CuO is exposed to H₂S gas at the temperature employed.

Received 14th June 2017
 Accepted 10th October 2017

DOI: 10.1039/c7ra06657k

rsc.li/rsc-advances

Introduction

Hydrogen sulphide (H₂S) is a “broad-spectrum” poison, namely it is toxic to several systems in the human body, however the nerve system is most affected. Enzymes that exist in the human body are capable of detoxifying H₂S by oxidation to harmless sulfates. However, the oxidative enzymes become overwhelmed when the H₂S concentration exceeds a certain threshold level of about 300–350 ppm on average.¹ To avoid harmful incidents occurring, the design of commercial H₂S gas sensors capable of detecting minute gas concentrations at ppm levels often requires a detection level as low as 5–15 ppm under moderate working temperatures. In this regard, chemiresistor-type sensors based on one-dimensional metal oxide semiconductors (MOSS) are attractive since they are capable of providing gas-sensing ability for the stable detection of trace amounts of hazardous gases with a wide range of chemical attributes. To detect H₂S gas specifically, various MOS sensing materials such as WO₃, SnO₂, ZnO, In₂O₃ and CuO have been explored.² The MOS sensors still suffer from major drawbacks such as cross-sensitivity, sensitivity to humidity, long-term signal drifting and slow sensor response.³ In particular, the poor selectivity remains a challenge to overcome and often limits their practical applicability.^{2–4}

In the literature, the gas-sensing properties of one-dimensional n-type vanadium pentoxide (V₂O₅) has seldom

been addressed, despite its promising potential in gas detection.^{5–10} Liu *et al.* first prepared V₂O₅ nanobelts decorated with either Fe₂O₃, TiO₂ or SnO₂ nanoparticles by a hydrothermal method.^{5,6} The hybrid nanobelts showed a moderately enhanced sensing response ($S = 2.0$ – 3.1 at 100 ppm ethanol) when compared to the pristine V₂O₅ nanobelts ($S = 1.7$) at 200 °C. Since then, V₂O₅ nanostructures have been investigated as gas sensors for detecting mostly organic vapours.^{7–10} Among them, Raible *et al.* reported a high sensitivity against organic amines such as 1-butylamine, with a detection limit as low as 30 ppb using V₂O₅ nanofibres.⁷ Raj *et al.* chemically prepared V₂O₅ nanostructures and found that V₂O₅ showed a slightly improved sensitivity toward ethanol at ppm levels compared to ammonia with identical concentrations at room temperature.^{8,9} Mondafferri *et al.* also demonstrated the sensing response against ammonia gas over a concentration range of 0.85–8.5 ppm at 200–250 °C using electrospun V₂O₅ nanofibres.¹⁰ Recently, the use of V₂O₅ nanostructures for the detection of inorganic, hazardous gases has begun to emerge.^{11–13} Yan *et al.* reported the room-temperature sensing capability of a porous silicon/V₂O₅ nanorod composite with a selective, substantially enhanced sensitivity toward NO₂ gas at low concentrations (3 ppm). This compares favourably to that of organic gases such as ethanol, methanol and acetone with an even higher concentration (100 ppm).¹¹ Mane *et al.* prepared V₂O₅ and Pd-decorated V₂O₅ nanorods on glass substrates by chemical spraying and subsequent thermal treatment.^{12,13} They also found an enhanced selectivity against NO₂ gas compared to other gases including NH₃, H₂S, CO, and SO₂.¹³

The use of V₂O₅ nanostructures as sensors for detecting inorganic toxic gases requires more work to assess their applicability. We herein report the decoration of CuO nanoparticles

^aDepartment of Materials Science and Engineering, National Chung Hsing University, Taichung 402, Taiwan. E-mail: wenjea@dragon.nchu.edu.tw

^bDepartment of Mechanical Engineering, National Chung Hsing University, Taichung 402, Taiwan. E-mail: gjwang@dragon.nchu.edu.tw

† Electronic supplementary information (ESI) available. See DOI: 10.1039/c7ra06657k



onto V_2O_5 nanowires to form hybrid nanostructures and investigate the gas sensitivity/selectivity of these nanostructures toward the toxic gases H_2S , CO and NO_2 . The reason for selecting CuO for the hybrid structure lies in the fact that there are reports about enhanced selective sensing achieved with p-type CuO semiconductors exposed to H_2S gas.^{14–17} For the first time, the CuO/V_2O_5 nanohybrids have been found to exhibit highly sensitive and selective detection toward H_2S gas at ppm levels continuously over a prolonged period of time (up to two weeks) and are relatively indifferent to CO and NO_2 gases over the moderate temperature range examined.

Results and discussion

Fig. 1(a) shows the morphology of the hydrothermally prepared V_2O_5 nanowires. V_2O_5 nanowires with a uniform diameter of 100 to 250 nm, a length of 10 to 20 μm and a smooth topography have been obtained. The XRD pattern in Fig. 1(b) shows characteristic diffraction peaks in good agreement with those of the orthorhombic V_2O_5 structure (JCPDS no. 41-1426). Fig. 2 shows that the V_2O_5 nanowires are of single crystal morphology. The lattice-fringe spacings in Fig. 2(b) are 0.434 and 0.343 nm, corresponding to the (001) and (110) planes of orthorhombic V_2O_5 , respectively. The nanowires grow along the [110] direction preferentially.

The V_2O_5 nanowires served as a backbone for the preparation of CuO/V_2O_5 hybrids with decorative CuO nanoparticles. Fig. 3(a) shows that the CuO nanoparticles with a diameter of

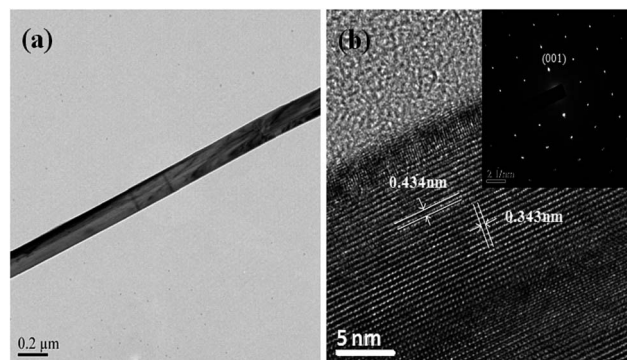


Fig. 2 (a) Bright-field TEM image, (b) HRTEM image and SAED pattern (inset) of a single V_2O_5 nanowire.

about 50 nm are well dispersed on the V_2O_5 surface. Fig. 3(b) shows a typical TEM bright-field image of the CuO/V_2O_5 hybrids, in which discrete CuO nanoparticles seem to adhere onto the V_2O_5 surface. The black dots are monoclinic CuO which was verified by TEM (Fig. S1 in the ESI†). Fig. 3(c) displays an XRD pattern of the CuO/V_2O_5 hybrids prepared *via* a deposition process, with a heat-treatment temperature of 400 °C. Well-defined crystalline phases have been found for the orthorhombic V_2O_5 and monoclinic CuO (JCPDS no. 48-1548), without the formation of any intermediate alloying compounds. It is worthwhile to note that the heat-treatment temperature turned out to be critically important for the successful preparation of CuO/V_2O_5 hybrids. If the temperature was raised to 500 °C, the hybrids became irregular fragments as shown in Fig. 3(d), suggesting that the V_2O_5 nanowires had partially melted or softened (note that the melting temperature of pure bulk V_2O_5 is about 690 °C) so the structure of the hybrid was destroyed.

Fig. 4 shows the sensing response of the pristine V_2O_5 and the CuO/V_2O_5 hybrid nanowires against 23 ppm H_2S gas over a temperature range from 100 to 380 °C. Two important findings have been observed. Firstly, the bell-shaped distribution reveals an optimum working temperature at which the sensing response is highest. This bell-shaped temperature dependence is ascribed to two main reasons.¹⁷ On the one hand, the adsorption, desorption and diffusion reactions involved, between the target gas and the semiconducting oxide surface, are all thermally activated processes. Hence the response increases with the working temperature.³ On the other hand, electrons in oxide semiconductors are more likely to attain sufficient energy to jump to the conduction band from the valence band at elevated temperatures. This leads to an increased concentration of free electrons so that electrical resistance is reduced accordingly. A combination of the thermally activated process, together with the increased probability of free-electron formation as the temperature was increased, results in an optimal temperature at which the electrical resistance (and hence the sensing response) is highest. In this regard, we have demonstrated for the first time that the optimal sensing temperature can be tailored to a lower temperature, against the model H_2S gas at ppm levels, through the decoration

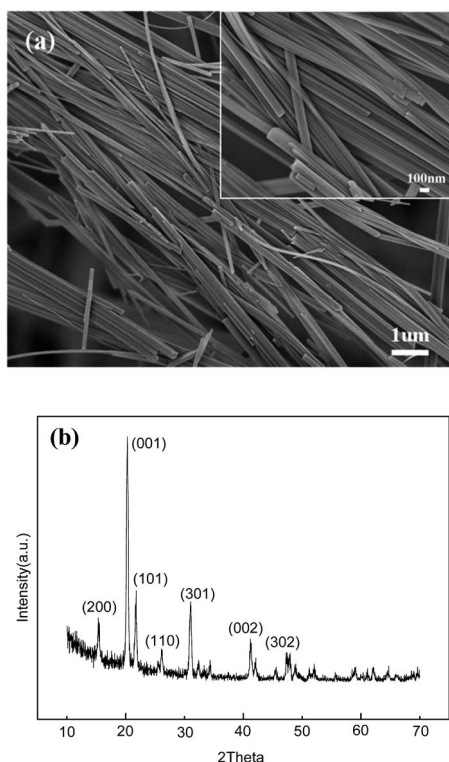


Fig. 1 (a) FE-SEM image and (b) XRD pattern of the hydrothermally prepared V_2O_5 nanowires.



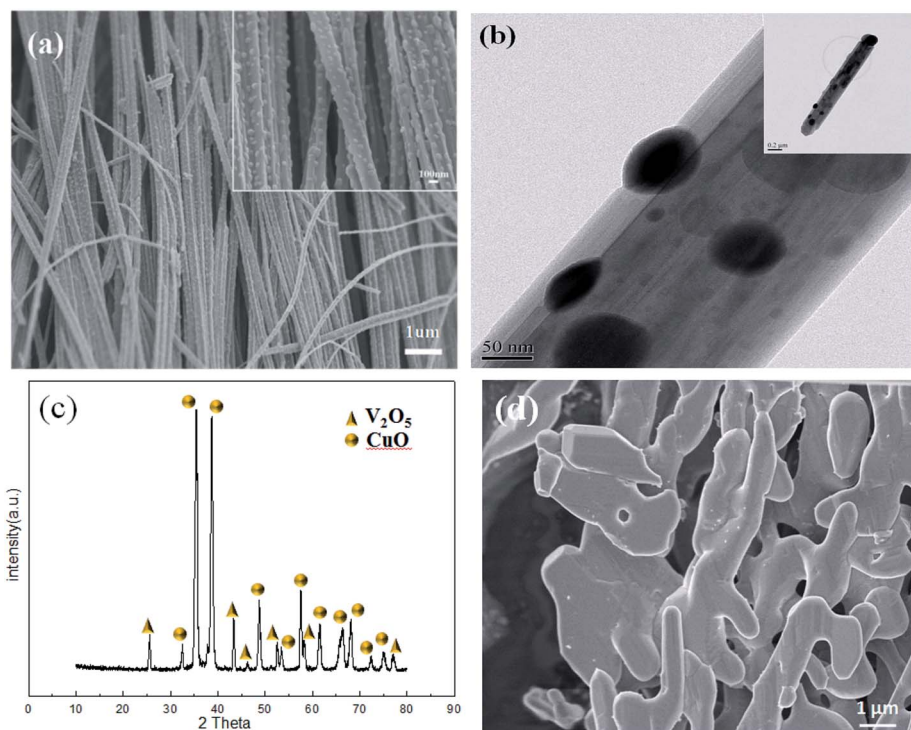


Fig. 3 (a) FE-SEM, (b) bright-field TEM and (c) XRD pattern of the CuO/V₂O₅ hybrids prepared at 400 °C. (d) FE-SEM image of the CuO/V₂O₅ hybrids prepared at 500 °C.

of CuO nanoparticles onto V₂O₅ nanowires in Fig. 4. Secondly, we have found that the CuO/V₂O₅ hybrids show a response as high as 31.86 against H₂S gas at ppm levels at 220 °C. For the first time, this compares favourably with that of the pristine V₂O₅, for which the highest response is merely 1.84 at 300 °C. The increased sensitivity is ascribed to the hybridization of V₂O₅ with the CuO nanoparticles together with the decorative hybrid structure, and will be discussed in later sections.

The CuO/V₂O₅ hybrid nanowires also display a significantly enhanced gas selectivity which is highly desirable in practical sensing applications. To illustrate this, the dynamic resistance behaviour of the pristine V₂O₅ nanowires is displayed in Fig. 5 against H₂S, CO, and NO₂ gases at 300 °C. Responses of the

V₂O₅ nanowires are 1.84 for 23 ppm H₂S gas, 1.48 for 60 ppm CO gas and 1.46 for 30 ppm NO₂ gas.

In addition, the response times toward detection of H₂S, CO, and NO₂ gases are 196, 174, and 212 s, respectively, as shown in Fig. 6(a–c), for the above gas concentrations. The sensing properties are primarily ascribed to the exchange of charge carriers between the adsorbed gas molecules and the V₂O₅ surface. In an air atmosphere, chemisorbed oxygen species, such as O²⁻, O⁻ and O₂⁻, trap electrons from the conduction band of the n-type V₂O₅ semiconductor, resulting in a space-charge depletion near the surface.¹⁸ After the introduction of the reducing H₂S or CO gas into the testing chamber, the gas molecules would react with the previously chemisorbed oxygen

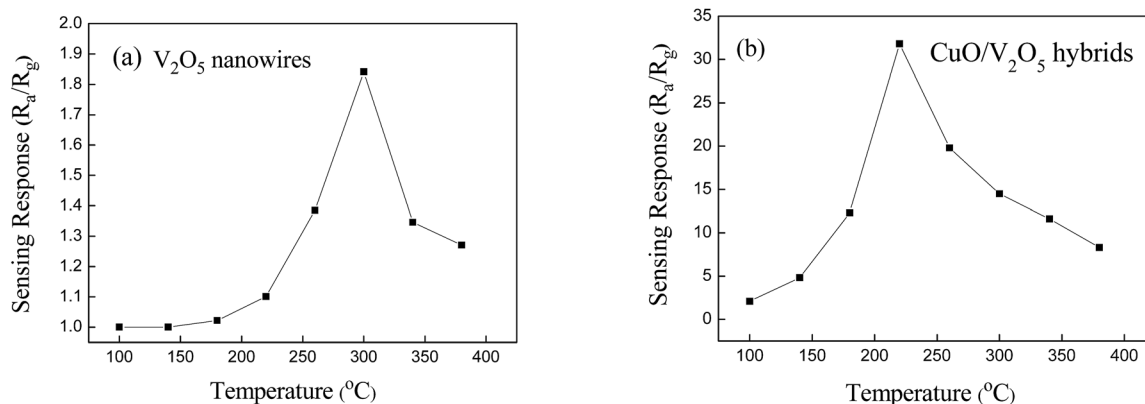


Fig. 4 Gas-sensing response of the (a) pristine V₂O₅ nanowires and (b) CuO/V₂O₅ hybrids against 23 ppm H₂S over a broad temperature range.



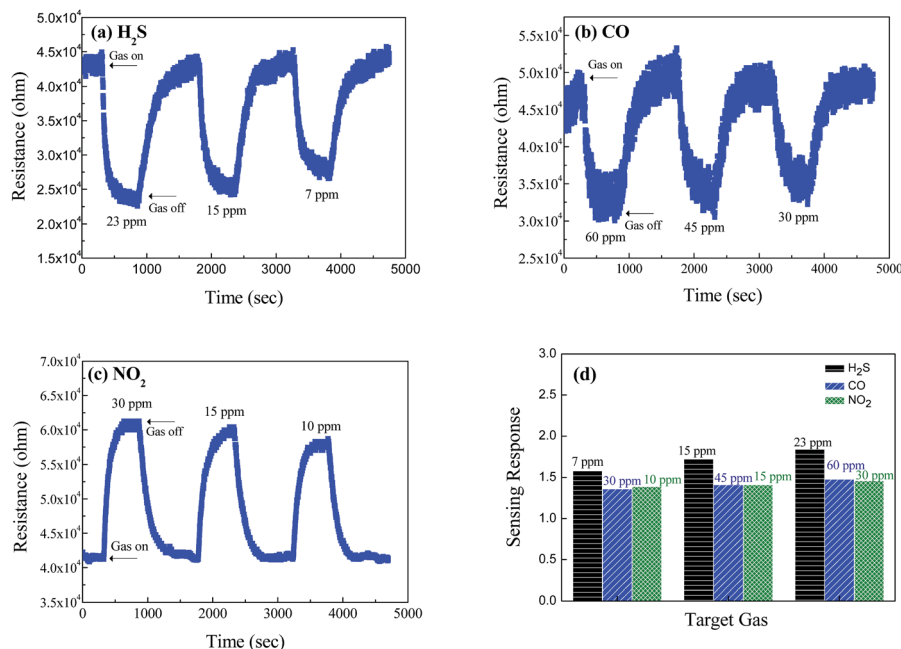
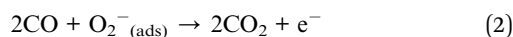
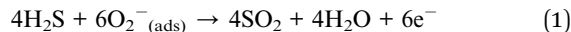


Fig. 5 Dynamic resistance change of the pristine V_2O_5 nanowire sensors against (a) H_2S , (b) CO and (c) NO_2 gases, at ppm-level concentrations at $300\text{ }^\circ\text{C}$. (d) A summary of the responses of the V_2O_5 nanowires against H_2S , CO , and NO_2 gas at $300\text{ }^\circ\text{C}$.

ions, so that the electrons trapped by the absorbed oxygen would subsequently be released into the bulk V_2O_5 nanowires, according to the following reactions (1) and (2):



This produces free electrons and hence decreases the electrical resistance. When the reducing gases were removed from the atmosphere, oxygen molecules spontaneously adsorb onto the V_2O_5 surface reversibly to trap free electrons, which causes the electrical resistance to increase, returning back to its initial value. In contrast, the adsorption of oxidizing NO_2 gas would

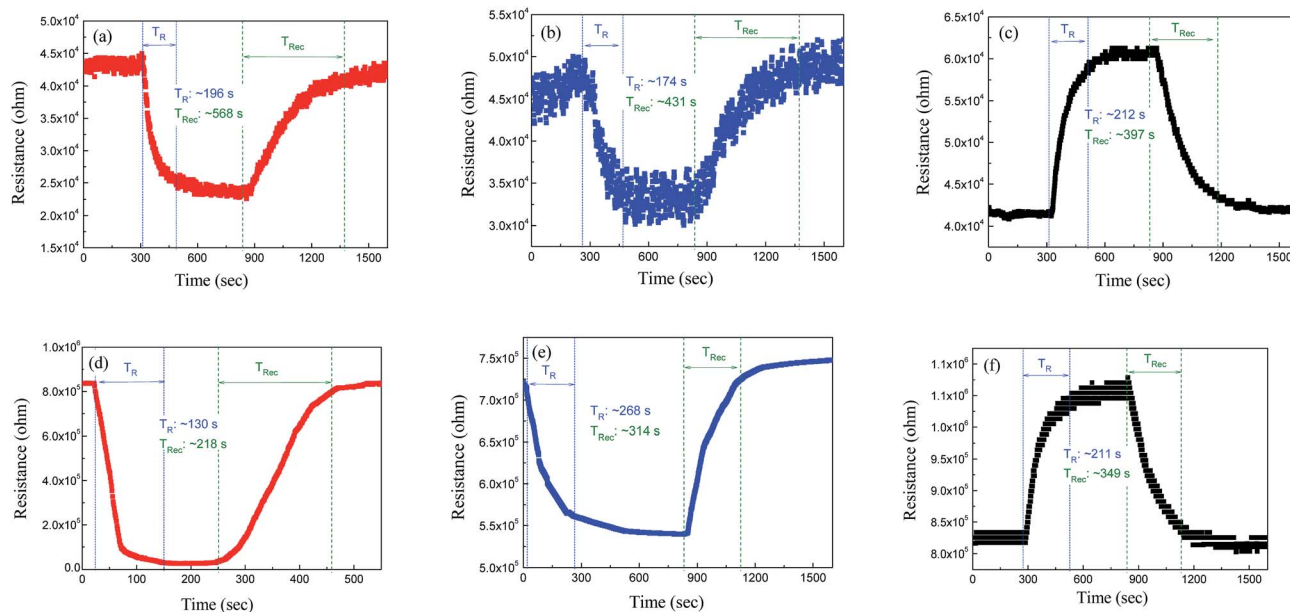


Fig. 6 Response time (T_R) and recovery time (T_{Rec}) of the pristine V_2O_5 nanowires against (a) H_2S (23 ppm), (b) CO (60 ppm) and (c) NO_2 (30 ppm) at $300\text{ }^\circ\text{C}$, respectively. T_R and T_{Rec} of the CuO/V_2O_5 hybrid nanowires against (d) H_2S (23 ppm), (e) CO (60 ppm) and (f) NO_2 (30 ppm) at $220\text{ }^\circ\text{C}$, respectively.



deplete the number of charge carriers in the surface layer of the V_2O_5 nanowires. This widens the depletion region, resulting in an increase in the electrical resistance accordingly. The desorption of gas molecules from the pristine V_2O_5 appears to be more difficult than the adsorption, so that a “tail” was found in Fig. 6(a–c).

In addition, Fig. 5(d) summarizes the sensing response of the pristine V_2O_5 nanowires. The lack of gas selectivity is apparent, however the sensor does provide a decent response to a change in concentration of the target gases over ppm concentrations, examined at the given working temperature.

Fig. 7 shows the dynamic resistance change of the CuO/V_2O_5 hybrids against H_2S , CO, and NO_2 gases. The responses of the hybrids are 1.33 against 60 ppm CO gas, and 1.29 against 30 ppm NO_2 gas at 220 °C. The result resembles that of the pristine V_2O_5 nanowires at 300 °C, despite the fact that the sensing temperature employed was reduced. A significantly enhanced sensing performance was found for the CuO/V_2O_5 hybrids toward H_2S gas selectively. Fig. 7(a) shows the resistance change of the CuO/V_2O_5 hybrids against H_2S gas of various concentrations at 220 °C; the responses are 31.86 at 23 ppm, 20.89 at 15 ppm and 7.86 at 7 ppm. This result indicates a dramatic enhancement of the sensing response from 1.84 for the pristine V_2O_5 nanowires to 31.86 for the CuO/V_2O_5 hybrids upon exposure to 23 ppm H_2S . Compared to the rather indifferent sensitivity of the hybrid nanowires against CO and NO_2 gases, a significantly increased sensing performance, nearly 18 times that of the pristine V_2O_5 nanowires, has been discovered toward H_2S gas selectively over the various gases and gas concentrations examined, as summarized in Fig. 8. Not to mention the fact that this occurs at a slightly lower working

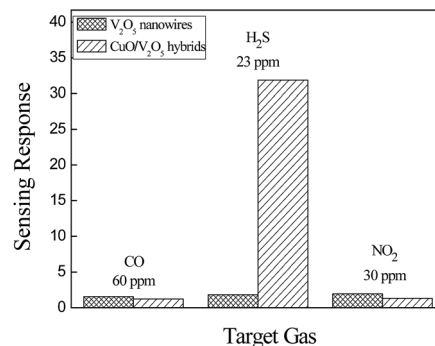


Fig. 8 Selectivity of V_2O_5 nanowires and CuO/V_2O_5 hybrids toward H_2S , CO and NO_2 gases at the optimal working temperature (300 °C for V_2O_5 , 220 °C for CuO/V_2O_5).

temperature (220 °C). In addition, Fig. 6(d) shows that the response time of the hybrid is 130 s for H_2S gas at a 23 ppm concentration. Therefore, the enhanced selective sensitivity is obtained with a simultaneously shortened response time. In comparison, the response times to detect CO and NO_2 gases are 268 and 211 s for the hybrids, respectively, which are similar to that of the pristine counterpart. Similar results have been found for the recovery times. The detection limit of the hybrid CuO/V_2O_5 nanowires has been determined experimentally, in which no response was detectable when the H_2S concentration was below 3 ppm.

The selective enhancement and increased sensitivity toward H_2S gas sensing of the CuO/V_2O_5 hybrids may be explained by the p–n junction formed at the dissimilar interface and

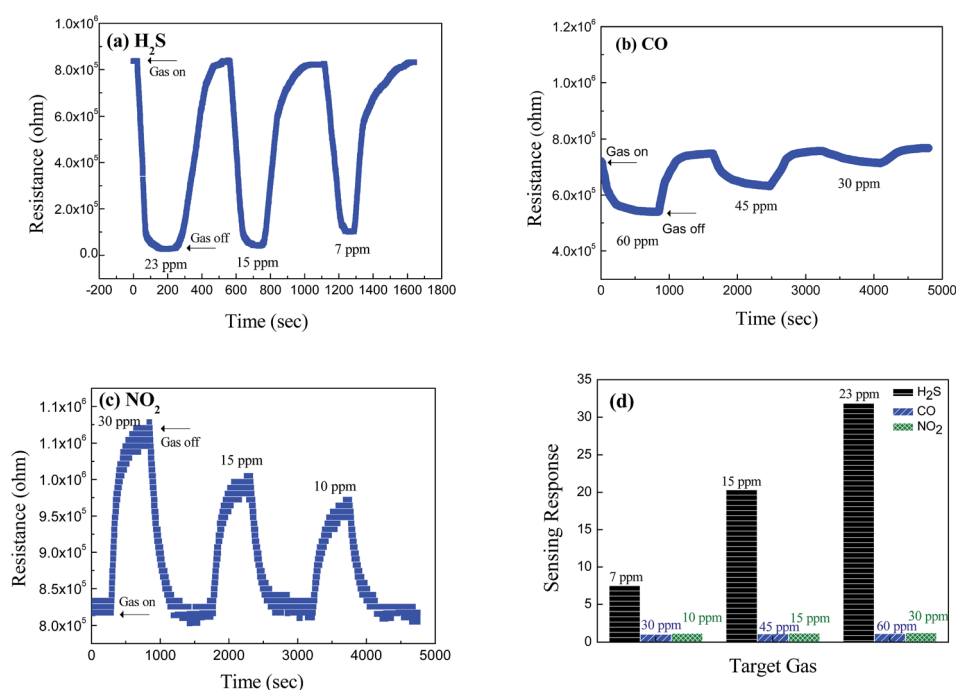


Fig. 7 Dynamic resistance change of the CuO/V_2O_5 hybrids against (a) H_2S , (b) CO and (c) NO_2 at ppm-level concentrations at 220 °C. (d) A summary of the gas response of the CuO/V_2O_5 hybrids against H_2S , CO and NO_2 at 220 °C.



sulfuration of the decorative CuO. The intrinsic V_2O_5 and CuO are n- and p-type semiconductors, respectively. The decoration of CuO onto V_2O_5 in the hybrids forms local p-n junctions at the interface.^{14-17,19,20} The width of the space-charge region (W) at the interface can be estimated from eqn (3) and (4) for n- V_2O_5 and p-CuO, respectively:^{20,21}

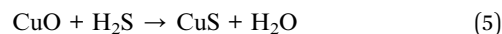
$$W_{V_2O_5} = \left[\frac{2\varepsilon_{V_2O_5} V_o}{q} \times \frac{N_{CuO}}{N_{V_2O_5}(N_{V_2O_5} + N_{CuO})} \right]^{1/2} \quad (3)$$

$$W_{CuO} = \left[\frac{2\varepsilon_{CuO} V_o}{q} \times \frac{N_{V_2O_5}}{N_{CuO}(N_{V_2O_5} + N_{CuO})} \right]^{1/2} \quad (4)$$

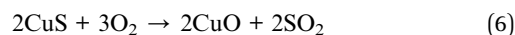
where ε is the permittivity (2.25×10^{-11} F m⁻¹ for V_2O_5 and 2.123×10^{-10} F m⁻¹ for CuO),^{20,22} V_o ($= 0.6$ eV) is the contact potential which is equal to the amount of the energy band bending between V_2O_5 and CuO ($\phi_{CuO} - \phi_{V_2O_5}$), q is the electrical charge of the carrier (1.6×10^{-19} C), and N is the carrier concentration ($N_{V_2O_5} = 1.48 \times 10^{18}$ cm⁻³ and $N_{CuO} = 1 \times 10^{19}$ cm⁻³, at room temperature).^{20,23} The calculated space-charge widths are 9.97 nm for V_2O_5 and 4.53 nm for CuO. These estimates are used for the plot of the energy-band diagram of CuO/ V_2O_5 p-n junction in air and H_2S , in Fig. 9(a). Energy-band bending at the interface is apparent. The band gap (E_g), electron affinity (χ) and work function (ϕ) of V_2O_5 are 2.3, 3.99, and 4.7 eV, respectively.^{24,25} Those of CuO are 1.35, 4.07, and 5.3 eV, respectively.²⁰ Note that the calculated space-charge widths are an estimate since the carrier concentrations used in the calculation are the values at room temperature. A more precise determination of the $W_{V_2O_5}$ and W_{CuO} needs information about the carrier concentrations at the working temperature (220 °C) employed. Nonetheless, the electrical transport channel is suppressed by the presence of local p-n junctions, according to the estimates of the space-charge region. This would hence lead to a higher base resistance (as observed in Fig. 6 where the base resistance values of the CuO/ V_2O_5 hybrids were 10 to 20 times greater than that of the pristine V_2O_5) and a larger change in electrical resistance (and hence sensing

response) for the CuO/ V_2O_5 hybrid nanowires compared to that of the pristine V_2O_5 counterpart.

An energy-band diagram shown in Fig. 9(b) further demonstrates how the sulfuration of the decorative CuO affects the response and recovery processes at the p-n junctions in the hybrids. In an air atmosphere, the potential barrier at the p-n junction impedes the electron flow through the interface. When H_2S gas is introduced into the testing chamber with a concentration exceeding a certain critical level (about 7 ppm determined experimentally in the present study), the CuO is spontaneously converted to CuS by the following chemical reaction:¹⁴⁻¹⁶



CuS is a metallic conductor, thus, the p-n junction as well as the charge-depletion region transform into a metal-n-type heterostructure. The potential barrier at the p-n junction is then expected to be lowered; therefore, the conversion from CuO to CuS facilitates the electron flow, leading to the drastic decrease in the electrical resistance. After the inflow of H_2S gas is terminated and air is re-introduced into the chamber, CuS changes back to CuO by oxidation:



The electrical resistance accordingly returns to its initial level. It may be interesting to note that the V_2O_5 surface, without being decorated by the CuO nanoparticles as in the CuO/ V_2O_5 hybrid, may also be involved in the gas sensing when H_2S is introduced. As yet, this appears not to contribute substantially to the H_2S selectivity.

The gas-sensing stability of the CuO/ V_2O_5 nanohybrids has been examined against 15 ppm H_2S for a long period of time. In Fig. 10, the sensing response remains relatively stable with an average sensitivity of 21.1 during the continuous two-week measurement. Note that every response value is in fact an average of seven measurements (as shown in the inset for the first data point). This finding indicates that the CuO/ V_2O_5

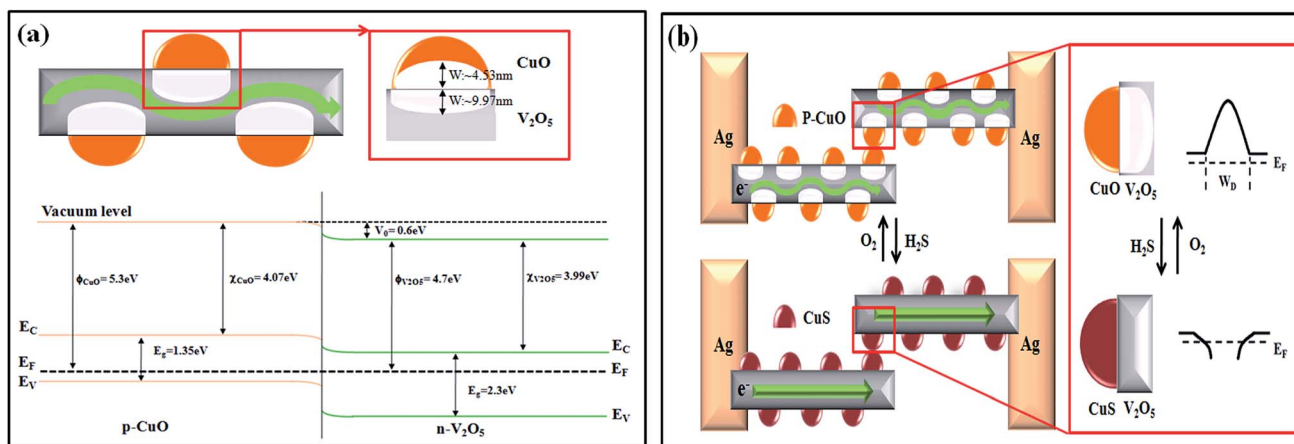


Fig. 9 (a) The band bending diagram and depletion-layer width at the p-n junction. (b) The energy-band diagram of the CuO/ V_2O_5 p-n junction in an air and H_2S gas atmosphere.



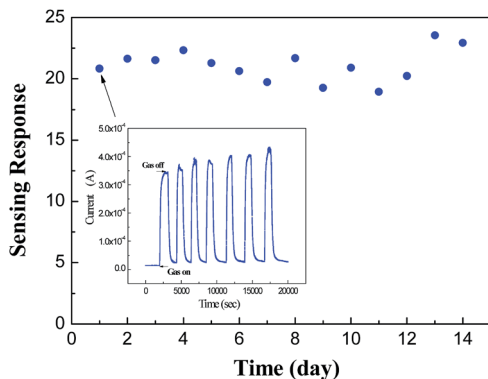


Fig. 10 Gas-sensing stability of the CuO/V₂O₅ nanohybrids against 15 ppm H₂S at 220 °C.

nanohybrids may be used in practical sensing applications for the selective detection of hazardous H₂S gas, despite more work being required to elucidate the applicability.

Experimental section

A. Materials

CuO-functionalized V₂O₅ nanowires were prepared by a facile two-step route, involving hydrothermal and wet-deposition processes. In the hydrothermal process, crystalline V₂O₅ nanowires were synthesized from a solution mixture consisting of 0.285 g V₂O₅ powder in 9 ml de-ionized water, with dropwise addition of 1 ml hydrogen peroxide (35%) under vigorous agitation for 1 h. The solution was then placed in a Teflon-lined stainless-steel autoclave and kept at 180 °C for 24 h before being cooled down to room temperature naturally. The resultant V₂O₅ nanowires were washed repeatedly with de-ionized water, centrifuged and then dried at 80 °C. In the wet-deposition process, the as-prepared V₂O₅ nanowires were dispersed in a mixed solution consisting of 10 ml of ethanol and 0.06 g of Cu(NO₃)₂·3H₂O. The suspension was then heated to 80 °C for the removal of ethanol. The powder was then placed in an alumina boat and fed into the centre of a three-zone horizontal quartz-tube furnace. The tube was first evacuated until the pressure inside reached 6×10^{-2} torr, before the introduction of a gaseous mixture containing 85 sccm argon (standard cubic centimetres per min at STP) and 15 sccm oxygen. The temperature was then increased to 400 °C with a heating rate of 20 °C per min and held isothermally for 1 h with a continuous flow of the mixed gas during the entire heating process to prepare CuO nanoparticles decorated on V₂O₅ nanowires.

B. Characterization

The morphology and crystalline structure of the V₂O₅ and CuO/V₂O₅ hybrid nanowires were examined by field-emission scanning electron microscopy (FE-SEM), X-ray diffractometry (XRD) with Cu K α radiation ($\lambda = 0.15405$ nm) and transmission electron microscopy (TEM).

C. Fabrication of the gas sensing devices

The gas sensors were fabricated by mixing the CuO/V₂O₅ hybrids or pristine V₂O₅ nanowires with methanol. The suspensions were then dispensed on alumina substrates with pre-configured, inter-digitated Ag electrodes. Analysis of the sensing properties was carried out in a self-assembled tubular furnace system along with a mass-flow controller, so that the concentration of various gases including air, H₂S, CO and NO₂ gases, could be precisely tuned. The electrical resistance was recorded by a volt-amperometric Keithley 2410 every 1 s over a wide range of gas concentrations (7 to 60 ppm) and working temperatures (100 to 400 °C) against target gases such as H₂S, CO and NO₂. For each test, the nanowire sensor was stabilized in air for 10 min before the target gas was introduced into the reaction chamber. The gas response (S) is defined as the ratio of the electrical resistance measured in fresh air (R_a) to the resistance measured in the presence of target gas (R_g). Either R_a/R_g or R_g/R_a was used for the determination of S , depending on the oxidising or reducing target gas used. The response time and recovery time are defined herein as the time it takes for the sensor to achieve 90% of its equilibrium level for the entire resistance change for adsorption and desorption of the target gas, respectively.

Conclusion

Hybrid p-CuO/n-V₂O₅ nanowires were prepared *via* a facile chemical route and their gas-sensing properties were investigated. The formation of local p–n junctions at the nanometre scale CuO/V₂O₅ interface, together with the reversible sulfuric/oxidative reactivity when exposed to cyclic H₂S gas/air at moderate temperatures, significantly enhanced the response and selectivity toward H₂S gas sensing. The hybrid nanowires showed a rather indifferent response when CO and NO₂ were used as the target gas. This unique selectivity toward H₂S gas at precise ppm levels means that hybrid p-CuO/n-V₂O₅ nanowires are anticipated to be used in a stable and reliable sensing device suitable for practical alarm applications.

Conflicts of interest

There are no conflicts to declare.

Acknowledgements

We would like to dedicate this article to the late Professor Yung-Chiun Her who has inspired many friends and students alike with his boundless spirit and enthusiasm. His greatness is not merely reflected by the amount of wisdom he gave in and out of classroom, but even more by the way he always practiced what he preached. This study was supported financially by the Ministry of Science and Technology (Taiwan) under contract no. NSC101-2221-E005-033-MY3. Experimental assistance from students at the National Taichung First Senior High School is also gratefully acknowledged.



References

- 1 S. Ramasamy, S. Singh, P. Taniere, M. J. S. Langman and M. C. Eggo, *Am. J. Physiol.: Gastrointest. Liver Physiol.*, 2006, **291**, 288–296.
- 2 V. E. Bochenkov and G. B. Sergeev, Sensitivity, selectivity, and stability of gas-sensitive metal-oxide nanostructures, in *Metal Oxide Nanostructures and Their Applications*, ed. A. Umar and Y.-B. Hahn, American Scientific Publishers, 2010, ch. 2, pp. 31–52.
- 3 H.-J. Kim and J.-H. Lee, *Sens. Actuators, B*, 2014, **192**, 607–627.
- 4 S. M. Kanan, O. M. El-Kadri, I. A. Abu-Yousef and M. C. Kanan, *Sensors*, 2009, **9**, 8158–8196.
- 5 J. Liu, X. Wang, Q. Peng and Y. Li, *Adv. Mater.*, 2005, **17**, 764–767.
- 6 J. Liu, X. Wang, Q. Peng and Y. Li, *Sens. Actuators, B*, 2006, **115**, 481–487.
- 7 I. Raible, M. Burghard, U. Schlecht, A. Yasuda and T. Vossmeier, *Sens. Actuators, B*, 2005, **106**, 730–735.
- 8 A. D. Raj, P. S. Kumar, Q. Yang and D. Mangalaraj, *Phys. E*, 2012, **44**, 1490–1494.
- 9 A. D. Raj, T. Pazhanivel, P. S. Kumar, D. Mangalaraj, D. Nataraj and N. Ponpandian, *Curr. Appl. Phys.*, 2010, **10**, 531–537.
- 10 V. Modafferi, G. Panzera, A. Donato, P. L. Antonucci, C. Cannilla, N. Donato, D. Spadaro and G. Neri, *Sens. Actuators, B*, 2012, **163**, 61–68.
- 11 W. Yan, M. Hu, D. Wang and C. Li, *Appl. Surf. Sci.*, 2015, **346**, 216–222.
- 12 A. A. Mane, M. P. Suryawanshi, J. H. Kim and A. V. Moholkar, *Appl. Surf. Sci.*, 2017, **403**, 540–550.
- 13 A. A. Mane, M. P. Suryawanshi, J. H. Kim and A. V. Moholkar, *J. Colloid Interface Sci.*, 2017, **495**, 53–60.
- 14 X. Xue, L. Xing, Y. Chen, S. Shi, Y. Wang and T. Wang, *J. Phys. Chem. C*, 2008, **112**, 12157–12160.
- 15 F. Shao, M. W. G. Hoffmann, J. D. Prades, R. Zamani, J. Arbiol, J. R. Morante, E. Varechkina, M. Rummyantseva, A. Gaskov, I. Giebelhaus, T. Fischer, S. Mathur and F. Hernández-Ramírez, *Sens. Actuators, B*, 2013, **181**, 130–135.
- 16 T.-S. Wang, Q.-S. Wang, C.-L. Zhu, Q.-Y. Ouyang, L.-H. Qi, C.-Y. Li, G. Xiao, P. Gao and Y.-J. Chen, *Sens. Actuators, B*, 2012, **171–172**, 256–262.
- 17 S. Ahlers, G. Müller and T. Doll, *Sens. Actuators, B*, 2005, **107**, 587–599.
- 18 R. Wang, S. Yang, R. Deng, W. Chen, Y. Liu, H. Zhang and G. S. Zakharova, *RSC Adv.*, 2015, **5**, 41050–41058.
- 19 Y.-C. Her, B.-Y. Yeh and S.-L. Huang, *ACS Appl. Mater. Interfaces*, 2014, **6**, 9150–9159.
- 20 S.-W. Choi, A. Katoch, J.-H. Kim and S. S. Kim, *J. Mater. Chem. C*, 2014, **2**, 8911–8917.
- 21 B. G. Streetman and S. K. Banerjee, in *Solid State Electronic Devices*, Pearson Education Inc., New Jersey, 2005, pp. 144–238.
- 22 R. M. Abdel-Latif, *Phys. B*, 1998, **254**, 273–276.
- 23 F. K. Butt, C. Cao, F. Idrees, M. Tahir, R. Hussain and A. Z. Alshemary, *New J. Chem.*, 2015, **39**, 5197–5202.
- 24 H.-J. Zhai and L.-S. Wang, *J. Chem. Phys.*, 2002, **117**, 7882–7888.
- 25 V. Shrotriya, G. Li, Y. Yao, C. Chu and Y. Yang, *Appl. Phys. Lett.*, 2006, **88**, 073508.

